

The Gaia Mission: Expected Applications to Asteroid Science

F. Mignard · A. Cellino · K. Muinonen · P. Tanga · M. Delbò · A. Dell’Oro · M. Granvik · D. Hestroffer · S. Mouret · W. Thuillot · J. Virtanen

Received: 10 December 2007 / Accepted: 10 December 2007 / Published online: 5 February 2008
© Springer Science+Business Media B.V. 2008

Abstract According to current plans of the European space agency, Gaia will be launched in 2011. By performing a systematic survey of the whole sky down to magnitude $V = 20$, this mission will provide a fundamental contribution in practically all branches of modern Astrophysics. Gaia will be able to survey with repeated observations spanning over 5 years several 100,000 s asteroids. It will directly measure sizes of about 1,000 objects, obtain the masses of about 100 of them, derive spin properties and overall shapes of more than 10,000 objects, yield much improved orbits and taxonomic classification for most of the observed sources. The final harvest will very likely include new discoveries of objects orbiting at heliocentric distances less than 1 AU. At the end of the mission, we will know average densities of about 100 objects belonging to all the major taxonomic classes, have a much more precise knowledge of the inventory and size and spin distributions of the population, of the distribution of taxonomic classes as a function of heliocentric distance, and of the dynamical and physical properties of dynamical families.

Keywords Asteroids · Astrometry · Photometry · Spectroscopy · Space-based observations

F. Mignard (✉) · P. Tanga · M. Delbò
Observatoire de la Côte d’Azur, Le Mont Gros, BP 4229, Nice Cedex 4 06304, France
e-mail: francois.mignard@obs-nice.fr

A. Cellino · M. Delbò · A. Dell’Oro
INAF – Osservatorio Astronomico di Torino, Pino Torinese, Italy

K. Muinonen · M. Granvik · J. Virtanen
Astronomical Observatory, University of Helsinki, Helsinki, Finland

D. Hestroffer · S. Mouret · W. Thuillot
IMCCE, Observatoire de Paris, Paris, France

1 Introduction

According to current plans of the European space agency (ESA), the Gaia mission will be launched around the end of 2011. This will be a major milestone for astronomical science because Gaia is expected to have a considerable impact on several branches of modern Astrophysics. As it stands Gaia is a very ambitious mission primarily designed as an upscaled version of one of the most successful ESA missions of the past years, namely the astrometric HIPPARCOS (HIGH Precision PARallax COLlecting Satellite) mission. But present technology makes it now possible to achieve astrometric performances that were a forbidden dream at the epoch of HIPPARCOS. Therefore, Gaia will reach an unprecedented astrometric accuracy, complemented also by excellent photometric and spectroscopic capabilities. In this way, Gaia will allow the astrophysicists to achieve a much better knowledge of our Galaxy, particularly for what concerns its kinematics, structure, history, distribution of stellar populations. In addition to this primary goal, Gaia will produce major contributions in the fields of stellar astrophysics, discovery of extra-solar planets, and fundamental physics including tests and measurements of parameters of primary importance in General Relativity.

In this paper, we focus on the results that are expected in Solar System science, with a particular emphasis on asteroid science. As will be clearly explained in the following sections, there are excellent reasons to believe that Gaia data will bring us into a completely new era of asteroid science: Gaia will produce direct measurements of asteroid masses and sizes, leading to new reliable estimates of average densities; it will derive orbits much more accurate than those computed by means of ground-based astrometric observations spanning over a couple of centuries; it will produce photometric data sufficient to derive the spin properties and overall shapes of a large sample of the whole population; and it will also derive a new taxonomy for many tens of thousands of objects. The Gaia legacy will be a new understanding of the asteroid population that will feed and trigger new ground-based investigations and space mission concepts for many years to come.

This paper, dealing with these various aspects of the Solar System science with Gaia, is organized as follows: after a general overview of the Gaia payload and a description of the focal plane assembly and the general observing strategy, we outline the asteroid signals that we expect to record on the focal plane. These are currently modeled by taking into account many subtle effects that will play a role in this complicated game. Then, a number of separate sections will be devoted to descriptions of the scientific results that are expected to come from the data collected by the different on-board instruments. The final section will be devoted to a general summary, and to a discussion of future developments.

2 Gaia Mission Overview

With a planned operational lifetime of five years, Gaia is expected to be one of the most impressive steps forward ever accomplished by stellar astrometry. At the end of 2011 according to current schedule, a Soyuz Fregat launcher will place the satellite into an orbit around the L2 Lagrangian point of the Earth, where it will start its scientific operations for an expected lifetime of five years. At present, the Gaia design has been finalized and the production process has been initiated by EADS Astrium.

The principles on which the mission is based are inherited from its notable predecessor, HIPPARCOS. This was another mission of the European space agency, launched in 1989

and completed in 1993. HIPPARCOS measured the positions of about 120,000 stars, all contained in an input catalogue, with a completeness limit around $V = 8$. Photometry in B and V bands was also accomplished. The typical astrometric accuracy of HIPPARCOS, 1 mas, represented a major advance over previously available catalogues. The observing strategy was based on a continuous sky scan over 2.5 years of operation, through two telescopes aiming at two fields 58° apart. The accuracy of the derived astrometry was made possible by carefully assuring the stability of that angle (the so-called “basic angle”) and by an appropriate knowledge, determined by the observations themselves, of the rotational phase of the satellite. In other words, the observed sources provided not only the requested scientific information (positions, parallaxes and proper motions), but were used also to reconstruct the probe attitude. To solve this problem, a self-consistent 3-step approach initially designed by L. Lindegren and based on a great-circles strategy was used (Lindegren 1976; Van Leeuwen 1997). Later, a new analysis based on a global iterative solution—-independent on great circles—was demonstrated to provide superior performances (Van Leeuwen 2005).

The latter approach will also be used for Gaia data reduction, since the astrometric mode of operation, based on the simultaneous observation of two different fields of view, is the same. However, recent technology improvements are exploited in the Gaia design, allowing a strong enhancement of the project ambitions. In Gaia, no input catalogue will be used, but all sources will be observed down to $V \sim 20$ (or $R \sim 21$). The total number of measured objects will thus rise up to about 1.3×10^9 .

The expected end-of-mission astrometric accuracy for single stars will reach $25 \mu\text{as}$ at $V = 15$, and $300 \mu\text{as}$ at $V = 20$. For sources brighter than $V = 12$ the accuracy will saturate at $7 \mu\text{as}$. In addition, Gaia will determine radial velocity at $2\text{--}10 \text{ km s}^{-1}$ level for stars with $V < 17$, obtain low resolution spectroscopy in the same brightness range and spectrophotometry in ~ 25 colours for $V < 20$. From these figures, it is clear that Gaia will offer an unprecedented accuracy in stellar astrometry and will be an innovating tool for studying both single objects and statistics of large samples. The astrometric information (position, proper motion, parallax) of each object will also be complemented by a number of fundamental physical properties (from photometry and spectrometry). This wealth of data will make it possible to map the Milky Way and its kinematics in three dimensions, and to address a large variety of open issues concerning, for instance, the distance indicators, the age of the Galaxy and of the Universe, the detection of extrasolar planets, the construction of reference frames and the determination of relativistic parameters.

This non-exhaustive list also includes Solar System objects. As we will see, several 10^5 asteroids (mainly in the Main Belt) will be repeatedly observed during the mission lifetime, but the data-set will also include planetary satellites, comets, near-Earth Asteroids and trans-neptunian Objects.

2.1 Mission Design and Operation

The Gaia satellite is built around a central structure containing all the main devices of the payload and service module, and surrounded by a large sunshield of nearly 10 m in diameter.

The optical elements and the focal plane assembly are mounted on a toroidal, polygonal structure. As shown in Fig. 1, two rectangular main mirrors, having a size of $1.45 \times 0.50 \text{ m}^2$ collect the signal coming from two viewing directions. The two light beams are then folded, recombined, and focused on the same focal plane instruments. The

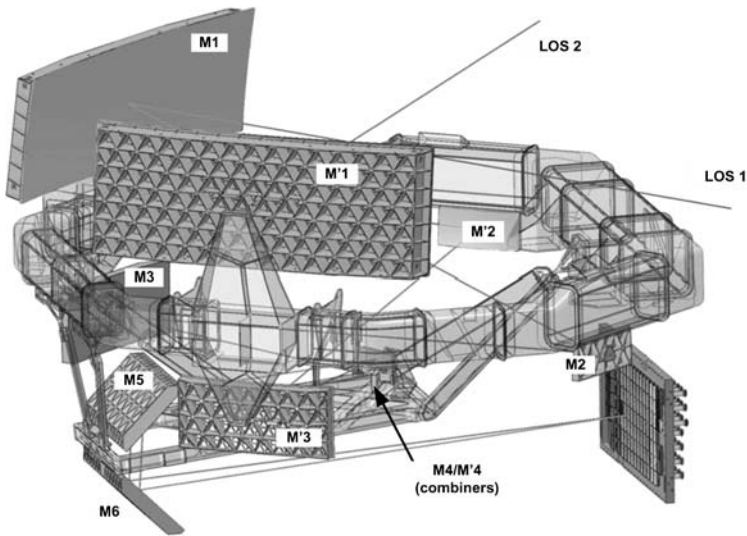


Fig. 1 The Gaia optical system, consisting of two lines-of-sight (LOS1 and LOS2), two main mirrors (M1 and M'1) plus several relay mirrors. In M4 beams are combined. The common focus is on the CCD array on the right

images of sources coming from both directions are mapped onto a common focal plane filled with a mosaic of CCDs. Thermal stability with passive monitoring is strictly required to provide the expected astrometric accuracy. We will briefly see how the processing chain can discriminate between sources coming from the two directions.

The spacecraft spins around an axis perpendicular to the toroidal focal plane assembly, with a rotation period of 6 h. In the absence of a precessional motion of the spin axis (see below) the two fields of view, being separated by 106.5° degrees, would thus sweep almost the same sky area at an interval of 106.5 min.

Figure 2 shows the structure of the huge matrix of CCDs, one of the largest ever made. All 106 CCDs have the same characteristics: 4500×1966 pixels, each pixel corresponding to 59×177 mas on the sky. In order to obtain images of the sources that are moving across the focal plane, the photoelectrons accumulated on the CCDs need to be transferred between adjacent pixel columns in such a way as to compensate the satellite rotational motion. To achieve this, the observation in time-delayed integration (TDI) mode is applied. In practice, the CCDs are read-out at a constant rate of $\sim 10^3$ pixels s^{-1} , corresponding to the angular rotation rate.

Data transmission bandwidth is the limiting factor for the quantity of data to be sent to Earth. As a consequence, only small patches of pixels data around every detected source (windows) will be transmitted. A set of possible windows differing in size has been defined, and each specific window is selected on-board from a pre-defined observation strategy for each source depending primarily on the apparent brightness.

In the scheme of Fig. 2, a star thus enters from the left, and drifts toward the right end, crossing the CCD columns marked by SM, AF, BP, RP, RVS in the order. When entering the field of view, a star is first detected by one of the two sky mappers (SM), each one receiving the light beam of one of the two viewing directions. The system then applies an appropriate observation tagging including the transit time (on-board timescale) and an identifier of the field of view. The SM information is then binned and stored in the mass

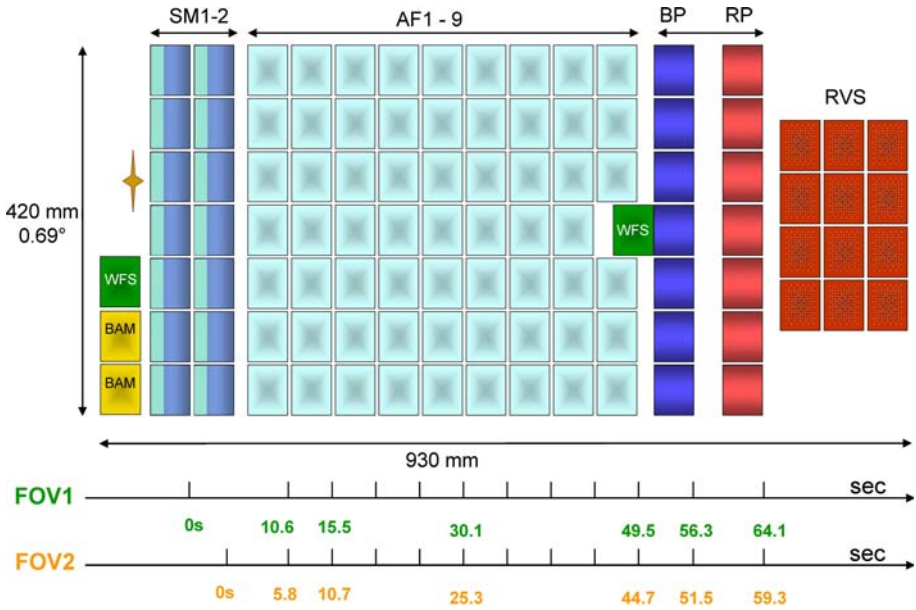


Fig. 2 The Gaia Focal Plane Array. Each rectangle indicates one CCD. The direction of star image motion is indicated at the bottom, with the time taken to reach different positions, relatively to the first detection in sky Mapper (SM) 1 (FOV1) or 2 (FOV2). The star image then crosses the main astrometric field (AF), the blue photometer (BP), the red photometer (RP) and the radial-velocity spectrograph (RVS). In addition, there are detectors for auxiliary instruments: the basic angle monitoring (BAM) system and the wavefront sensors (WFS). In this figure the “across-scan” (AC) and “along-scan” (AL) directions defined in the text are vertical and horizontal, respectively. (See TBD for color version)

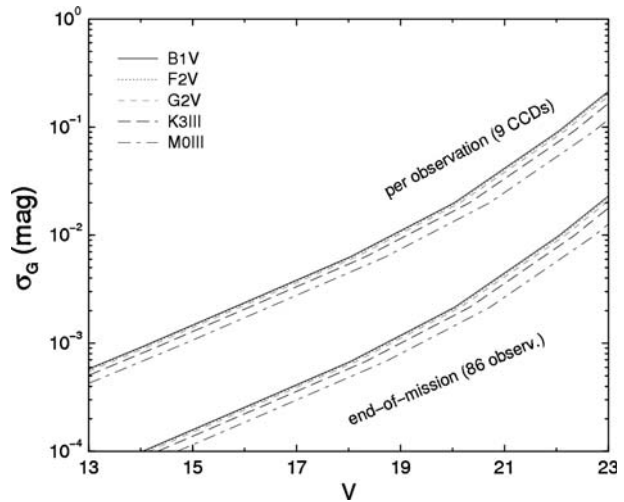
memory. For stars with $V > 13$ a window of 4.7×2.1 arcsec is transmitted, with pixels binned 4×4 . A double window size is transmitted if the star is brighter.

Afterwards, the star drifts across the astrometric field (AF), progressively feeding each of the nine columns of AF CCDs. Based on the previous SM detection, the system carries out an on-board centroiding that allows one to assign the window positions in each AF CCD. As for the SM, AF window sizes depend upon the source brightness. The details of windowing are rather complex and have been chosen keeping in mind constraints coming from telemetry, CCD saturation, signal sampling, background measurement and star density.

It must be noted that for stars brighter than $V \sim 13$ “gates” are activated on the AF CCDs to deal with the saturation of the wells. This means that the charge is emptied from the CCD by a gate before it reaches the final read-out register. The effect is a reduction of the exposure time, depending upon the position of the activated gate among the 12 possible options. In this way, stars as bright as about $V = 4$ can be observed without saturation.

For sources fainter than $V = 13$, a binning perpendicular to the scan direction (“across scan”, AC) is always performed. As a consequence, full single-pixel resolution is only available “along scan” (AL). On the other hand, for $V < 13$ a fully resolved, 2D window is read and transmitted. In all cases, the window size is not larger than 1.1 arcsec in the Along-scan (AL) direction (0.7 arcsec as for $V > 16$), and 2.1 arcsec in the Across-scan (AC) direction. Therefore, the AF instrument delivers in any case the best possible astrometric information.

Fig. 3 Estimated precision of the G magnitude, as a function of V, per focal plane transit and at the end of the mission without the calibration errors



As for the wavelengths response of the AF CCDs, it behaves as an unfiltered, Silicon-based device. The photometric broad passband has been named “G-band”, after “Gaia”.

Sources fainter than $G = 20$ (i.e., $V \sim 20\text{--}21$ depending upon color) are not selected by SM for window assignment and further observing.

The photometric precision expected for the AF detectors is also very good (Fig. 3). With a typical uncertainty of 10^{-3} mag for each transit on the focal plane, it is clear that the limiting factor will be calibration.

The spectrophotometric capability of Gaia comes from the blue photometer (BP) and the red photometer (RP). These are two CCD columns covered by a blue and a red filter, respectively. The light beam reaches them after having being dispersed by a prism, thus providing spectra at a resolution of 3–29 nm/pixel for BP and 7–12 nm/pixel for RP. In the case of Solar System objects, these data will constitute a valuable source for building a completely revised taxonomic classification for asteroids.

The radial velocity spectrometer (RVS) is a near IR (847–874 nm) spectrograph of medium resolution ($R = 11500$). It has been designed in order to provide details about a spectral region reach of features allowing to study rotational velocities, atmospheric parameters (effective temperature, surface gravity, metallicity), and abundances of chemicals relevant for tracing the Galaxy evolution. Its interest for Solar System science is very limited, and in fact goes the other way round with the use of bright Solar System objects to calibrate the instrument by using the known radial velocities and the Sun spectral features that can be observed in their flux. No specific Solar System science will probably be derived with this instrument.

2.1.1 Observing Strategy

The satellite will operate by continuously scanning the sky, for 5 years. The scan motion is granted by the spin with a period of 6 h. But this is only one of the three rotational motions imposed to the spacecraft.

The other two components are (i) a precession of the spin axis (with a period of 63 days), and (ii) a change in orientation of the precession cone axis over one year.

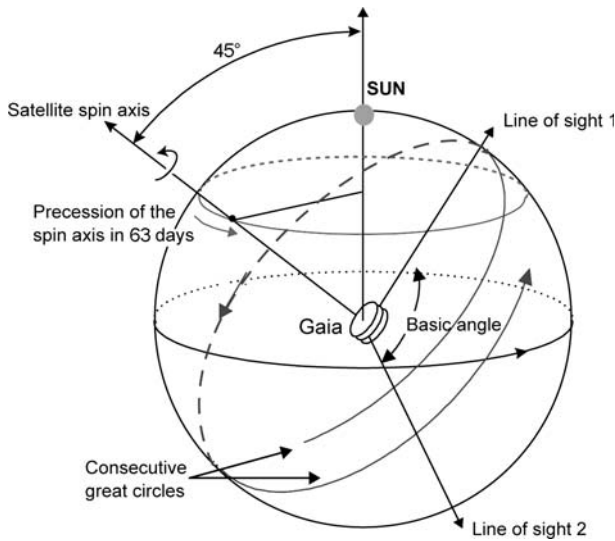


Fig. 4 The Gaia scanning law is illustrated on this scheme of the celestial sphere. The scan movement is the result of the combination of three rotations: satellite rotation (period of 6 h); spin axis precession; annual revolution around the Sun

This last rotation is due to the fact that the precession cone axis is always pointed toward the Sun. The spin axis makes an angle of 45° with the Sun direction, a feature which constrains seriously the geometry of observations of Solar System sources as explained below. The overall picture of the scanning is shown in Fig. 4.

The combination of the three motions allows to gradually shift the scan circle over the sky. In this way, 86 observations for each source will be obtained, on average, in 5 years. The number of scans on the sky, as function of ecliptic latitude, is illustrated in Fig. 5. Close to the ecliptic, where most of Solar System objects are found, the number of observations is slightly smaller with typically 50–60 transits. (See TBD for color version.)

2.2 Solar System Observations

By estimating the completeness level of the current sample of asteroids, we can evaluate that the number of asteroids that Gaia will observe assuming a magnitude limit $V \sim 20$ will be about 3×10^5 . Most of them will be known at the time Gaia flies, and even several objects on peculiar orbits (for example: high inclinations) will be detected before by all-sky survey that are expected to come into operation in the near future (like Pan-STARRS). A weak discovery potential will probably survive, mainly concerning Inner Earth Objects that are hardly observable from Earth. It is clear however that physical and dynamical characterisation are the strong points for Gaia, and not discovery.

To asteroids, we should then add comets and natural planetary satellites. Larger objects will be excluded from direct detection as explained at the end of this section.

The particular geometry of the scan movement prevents the Gaia telescopes to be pointed in cone centered either on the Sun, or at opposition. On the other hand, the scanning circle crosses the ecliptic plane approximately around quadrature, at 90° solar

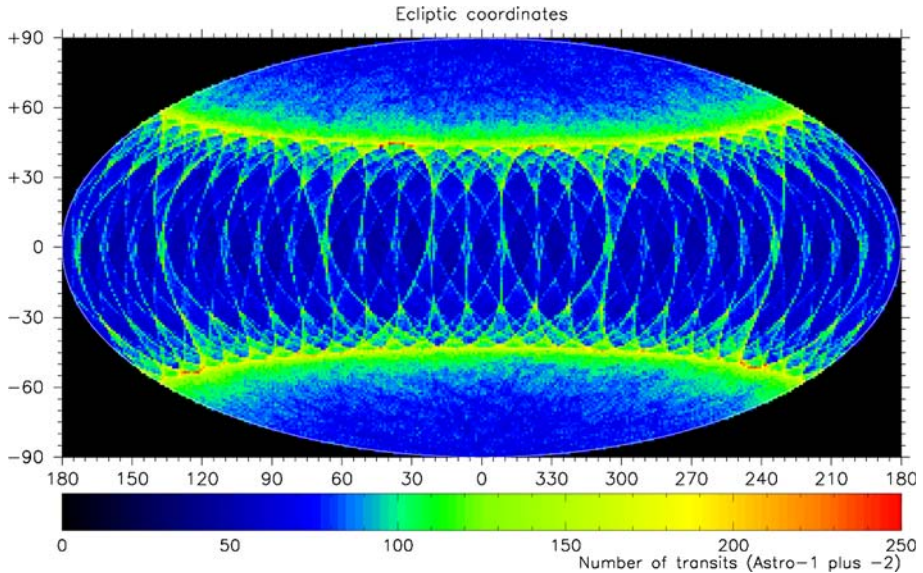


Fig. 5 Number of observations on the sky, in ecliptic coordinates

elongation. To be precise, the observable region extends from 45 to 135° of elongation, in both directions (Fig. 6).

Two main consequences result from this geometry. First, the observations of Solar System objects occur, most of the times, in sequences separated by non-observable periods extending over three to six weeks. In fact, during one precession cycle (63 days) the scan circle sweeps twice the observable elongations, collecting several transits of a typical, slowly moving asteroid (very nearby NEOs excluded for the moment) that is inside the visibility zone. Conversely, when the same object lies in the unreachable sector, it spends there the time necessary to cross it, following its orbital motion, and the revolution of Gaia (and the Earth) around the Sun. The second consequence is the relatively high phase angle with which a typical asteroid is observed and the total lack of observations around conjunctions and oppositions. As we will see, this fact has some consequences on data reduction and exploitation.

The apparent velocity of an asteroid when it enters the field of view will be distributed as shown in Fig. 7. A window assigned at the beginning of the transit, that is propagated in the AF field assuming that a “fixed” star is observed, will not be large enough, in many cases, to have the signal peak centred all over the transit. In fact, the median velocity AL for a main-belt object is ~ 7 mas/s, and ~ 30 mas/s for NEOs.

Since about 50 s separate the detection in SM1/2 from the end of transit in AF, it is clear that an object can reach and cross the edge window by drifting more than 6 pixels (360 mas AL) relatively to the window centre (the AC displacement is less relevant, since the window is larger in that direction). For this reason, in order to avoid a large loss of asteroid observations, a specific strategy will be adopted for those objects whose velocity, as estimated by position difference in SM and AF1, will be above a certain threshold. The problem of adapting the window propagation speed to the detected displacement is that a very small fraction of false movement detections (for example, for double stars with a companion at the detection limit) could result in a very high number

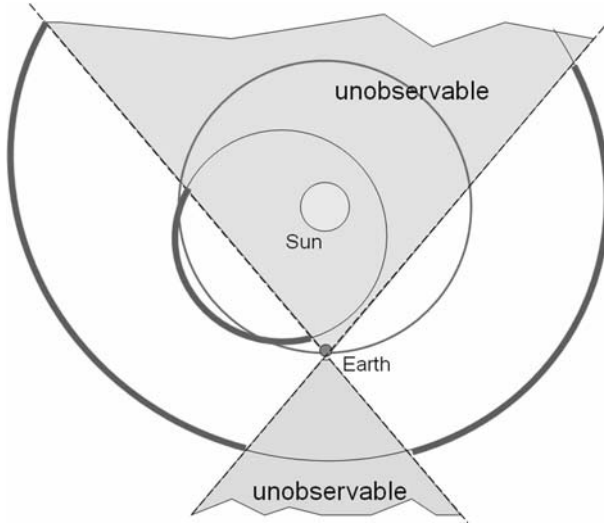


Fig. 6 The region not reached by Gaia, projected on the ecliptic, relative to Earth and Sun positions (shaded regions). The red arcs represent an example of observable orbit segments for a main-belt and a near-Earth asteroids. This picture is only meaningful at a particular time and as the Earth moves on its orbit the whole pattern is rotated and observations are performed on previously unseen parts of the asteroid orbit

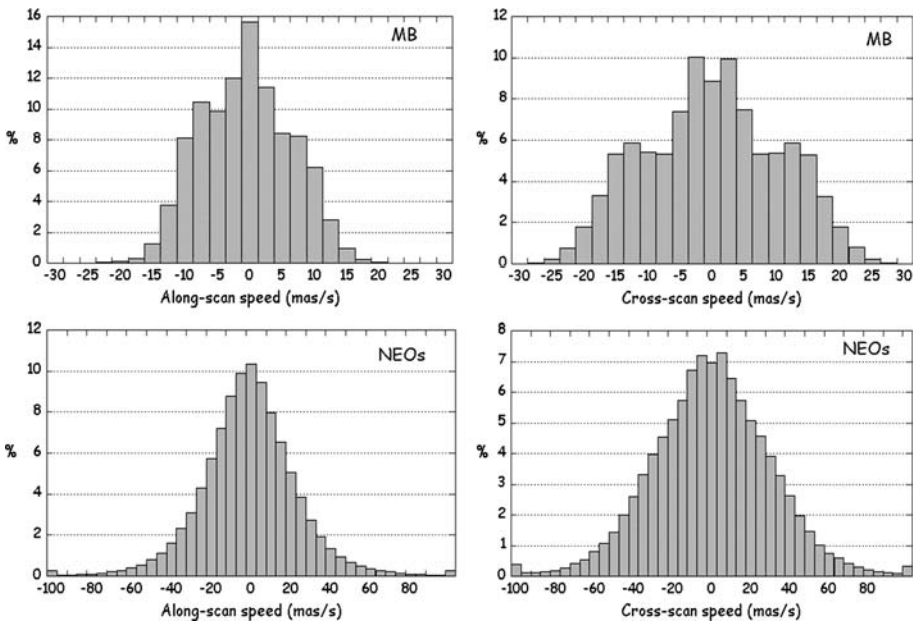


Fig. 7 The four panels represent the speed distribution as measured on the focal plane, relative to stars, of Main Belt (MB, left column) and Near Earth Objects (NEO, right), along scan (top row) and across (bottom). The plot is built by running a simulation of detection over 20000 objects

of stars that are lost during transit. In fact, due to the high ratio between the expected star and asteroid population (a factor $\sim 1.5 \times 10^9 / 3 \times 10^5 = 5 \times 10^3$) the loss of stars during transits will be much higher than the gain in asteroid observations. It was thus proposed that fast moving objects should be assigned two windows: one moving as a nominal, fixed object window, and the other moving at the estimated velocity. In this way the problem of false displacement detections is overcome without side effect on star observations.

The window assignment process coupled with the electronic data handling performed on-board has another consequence on Gaia observations of Solar System objects. Most notably, large extended objects (major planets) cannot be observed. The current system design does not allow detection of sources of angular size larger than ~ 200 mas, for which a photocentre position cannot be reliably determined by the on-board processing. This is not a serious drawback for minor planets, with just a handful of bodies affected.

Performances on extended objects presenting a sharp luminosity peak (such as active comets with a developed coma) are still under evaluation.

3 Analysis of Asteroid Signals

The big advantage of Gaia, with respect to ground-based telescopes of larger aperture, will be obviously the fact of being diffraction-limited. The image of an object on the GAIA focal plane is the result of the convolution of the incoming wave front with the optical system of GAIA, described by the point spread function (PSF) of the instrument. The PSF contains all information about the optical response of the GAIA telescope, depending on the position on the focal plane and the spectral properties of the source. Since the satellite rotates around its spinning axis, any detected celestial source transits across the Gaia focal plane, and its optical signal is recorded by a series of CCDs and converted into an electronic signal consisting of a distribution of photoelectrons generated in the CCD pixels. The signal is recorded by applying a TDI (time delayed integration) acquisition mode, that is optimized to keep any non-moving source in rest within each CCD during its transit across the focal plane. In general, and depending on the apparent magnitude of the source, the optical signal is not only digitized by the CCD pixels, but it is also integrated along the across-scan direction, leaving only information in the along-scan direction (Fig 8).

In order to predict the properties of asteroid signals on the Gaia focal plane, it is necessary to model some intrinsic properties of the incoming object images. First of all, the angular size and the shape of the asteroid play a dominant role in the feature of the final image. In particular, the width of the produced signal will be used, when possible, to derive the apparent angular size of the asteroid (see Sect. 4). Less important, but not negligible at all, are the optical scattering properties of the surfaces. The reason is that the radiation by an asteroid at visible wavelengths consists of sunlight scattered by the surface. The exact flux of photons incident on the Gaia focal plane will then be the final result of a complex interaction of solar photons with the asteroid surface. The object's size, albedo, shape, macroscopic and microscopic roughness, and light-scattering properties will all play a role in the final properties of the recorded signal. This complex process is currently not fully tractable by means of purely analytic means, and no definitive theory of light scattering is presently available, although several models describing the most general properties of realistic light scattering properties are available.

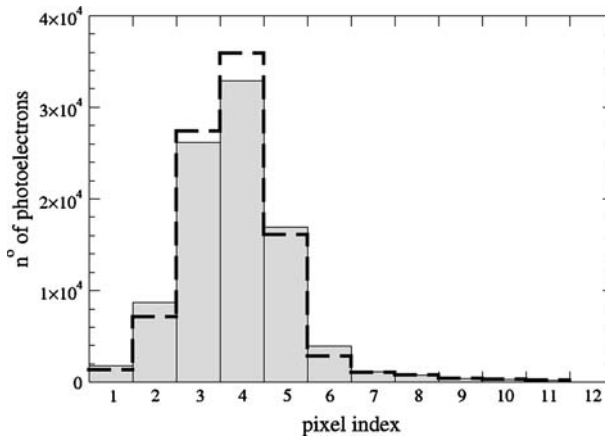


Fig. 8 Example of a simulated asteroid signal on one of the astrometric CCDs on the focal plane, according to the following parameters: window size: 12 px; apparent angular size: 120 mas; apparent magnitude: 14. As a comparison, the Figure shows the predicted signal (bold-dashed contour) for a point-like source having the same apparent magnitude and position in the CCD. Given the scale chosen for the y-axis, it is easy to see that the differences are very relevant

As opposite to the case of “fixed” stars and other non-moving astrophysical sources, the apparent motion of the asteroids across the celestial sphere has a very important role in the formation of the final signal on the focal plane. The apparent motion of the asteroids will be the first characteristic of the signal of these objects that will be identified along the Gaia data reduction pipeline. Sources identified as non point-like (producing signals definitely different from the theoretical PSF of a point-like source), and/or moving during the transit on the Gaia focal plane, will be immediately removed from the main data pipeline, and kept apart to be sent to a different branch of the pipeline, in order to apply to them specific data reduction algorithms.

The asteroid velocity, and mainly the along-scan velocity, introduces an additional spreading of the optical signal on the CCD detectors, which is not corrected by the TDI mode of operation of the CCDs. In other words, the proper motion of a source affects the signal in such a way that it can be confused with the signal of a non-moving source, but with a larger angular size. It follows that the knowledge of the source’s velocity is crucial point for asteroid signal analysis. The detection and accurate measurement of the apparent motion, is also a very valuable piece of information to constrain the orbit determination (see Sect. 7).

After removal of the effects related to finite size and motion, the main source of noise affecting the final signal is the magnitude-dependent photon noise. However, several other subtle effects will play a role in the generation of the final signal recorded by the detectors, depending on the instrument’s characteristics. An example is given by the electronic noise in the read-out of the CCD counts. The time-delayed integration mode of the CCDs introduces an additional spreading of the signal, and also a systematic shift of the apparent photocenter (Bastian and Biermann 2005) in the along-scan direction. Other distortions are introduced by charge diffusion on the CCDs and non-ideal efficiency of the charge transfer in the TDI mode. This is expected to produce a sort of charge entrapment and a spurious “tail” in the final signal. All these effects are being deeply investigated in order to provide a correct interpretation of the Gaia signals.

4 Measurement of Asteroid Sizes

Asteroids are not point-like sources, therefore it is certain that, above some given limit of apparent angular size, and depending also on the apparent magnitude at the epoch of observation, an asteroid signal produced on the Gaia focal plane will be different with respect to the ideal case of an unresolved star. An extensive analysis has been carried out to predict in quantitative terms what will be the above limit in angular size, as a function of magnitude, for which a direct measurement of the apparent sizes of the objects, or, more precisely, of their projections along the along-scan direction in the focal plane, will be possible. An earlier summary of this subject is given by Dell’Oro and Cellino (2005).

As explained in Sects. 2 and 3, in general the asteroid signals will consist of distributions of photoelectrons produced on the focal plane. These photoelectrons will be generally collected in a series of CCD pixel columns perpendicular to the along-scan direction of the satellite, therefore the final signals will consist of a series of numbers, corresponding to the amounts of photoelectrons collected in each bin. These signals will be characterized by few parameters, like a brightness peak, a width, a photocenter, corresponding, roughly speaking, to the location of the median of the received photoelectron distribution, and an integral, corresponding to the disk-integrated brightness of the observed object. The basic idea is then to use the above properties of the signal to derive information on the along-scan apparent angular sizes of the detected targets. In particular, the width of the signal is used for these purposes. The analysis is iteratively performed at different degrees of approximation. At the lowest level, the signal is assumed to be created by an object having a spherical shape, moving in the sky at a given rate, and seen at zero phase angle (the phase angle being the angle between the directions to the Earth and to the Sun, as seen from the asteroid). This is also the first, preliminary analysis of the signal that is performed just after receiving it in the branch of the data reduction pipeline that will be followed by sources whose signals do not fit those of “fixed” single stars, and are then immediately removed from the main pipeline. When the source is an already known Solar System object, the phase angle at the epoch of detection is then also known, and this can be included in the model that makes a prediction of the signal from an extended spherical source, and compares this with the properties of the collected signal. In particular, the simple idea is that the signal width is diagnostic of the along-scan angular size of the source. Given the measured signal width, the algorithm determines the angular sizes of a spherical source observed under the same observing circumstances. Unfortunately, due to photon statistics, the relation signal width—size is not one-to-one even with the simplifying assumption of spherical objects. Due to photon statistics, any given object observed in the same conditions several times, will not produce the same signal at each detection. Therefore, to any given observed signal width one can associate a range of possible angular sizes compatible with the observed signal. Of course, the range of possible signal widths corresponding to a given angular size (or vice versa) being an effect of photon statistic, is a function of the apparent magnitude (i.e., of the number of collected photoelectrons) of the object. Brighter objects have associated angular size uncertainties much smaller than fainter objects of the same angular size. The situation is then fairly complicated, but can be quantitatively analyzed by means of extensive simulations.

In particular, simulations allowed us to identify, in a plot of the plane apparent magnitude—angular size, the domain for which a size measurement having an intrinsic uncertainty below a given limit can be carried out. In particular, by choosing an uncertainty limit of 10%, it is possible to show what is the minimum apparent brightness required to resolve objects as a function of their apparent angular size.

The results of these simulations can be better interpreted by complementing them with detailed predictions of the detections of known main-belt asteroids in a simulated Gaia survey mimicking five years of operational lifetime. According to the simulations, each main-belt asteroid will be observed many times (the average number of detections being 65) during the mission. Successive detections will occur in different sky locations, and different observing circumstances (heliocentric and geocentric distances, apparent magnitude, phase angle, etc.). For each observation, we can establish the predicted accuracy of a size measurement, based on the results of the analysis described above. In this way, we can derive an evaluation of the performances of Gaia in deriving direct measurements of angular sizes for main-belt asteroids (and in principle also for near-Earth asteroids, although no quantitative analysis concerning these objects has been done, yet).

The results of the simulations shown in Fig. 9 indicate that above a size of 30 km in diameter, more than 50% of the known main-belt asteroids will have their size measured at least once during the Gaia operational lifetime with an accuracy better than 10%. The number of useful measurements rapidly increases for increasing size. Between 20 and 30 km, a fraction larger than 20% of the objects will also be measured at least once, or even a few times.

We note also that the procedure of size measurements is inherently iterative, and is strongly linked with other branches of the overall data reduction pipeline. In particular, the assumption of a spherical shape is a zero-order assumption that is subsequently replaced by more realistic shape models during the process of data reduction. In particular, taking

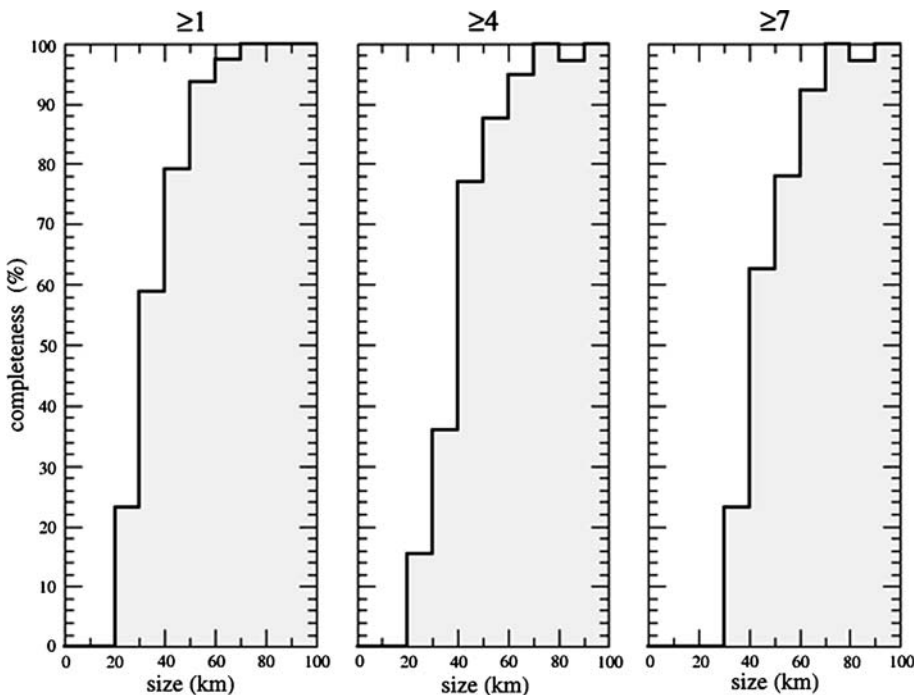


Fig. 9 Predicted percentage of the existing main-belt asteroids that will have their apparent angular sizes measured by Gaia with an accuracy better than 10% at least once, four and seven times (from left to right) during the Gaia operational lifetime, as a function of their actual sizes (see text)

advantage of the results of the disk-integrated brightness data (see Sect. 5), the initial spherical assumption will be replaced by a triaxial ellipsoid approximation in agreement with the results of brightness inversion. Different iterations of the size measurement procedure are also strictly related to a progressive improvement of the interpretation of the signals collected at each transit of an asteroid on the Gaia focal plane. In particular, the overall solution for size and shape of the objects will also produce an improved estimate of the predicted shift of the measured photocenter of the signal with respect to the projection of the object's center of mass on the Gaia focal plane. This information will be of the highest importance in order to improve the performances of orbit determination for the objects, from which also further information like mass, will be obtained (Sects. 7 and 8).

According to current simulations, the number of objects for which we can predict to be able to obtain a direct size measurement is thus of the order of 1,000, and will represent a huge improvement of the very limited data-base of asteroids with sizes directly measured, and not derived by means of indirect techniques, like thermal radiometry and polarimetry. The availability of this Gaia data-base of asteroid sizes will be very important for our knowledge of the size distribution of the asteroid population, which is an essential source of information for the studies of collisional evolution of the asteroid population. We note that this result will not be possible in the foreseeable future by using any other observing facilities, including the new telescopes that will be soon in operation and will be devoted to perform extensive sky surveys.

5 Disk-integrated Photometry

As seen in previous Sections, main-belt asteroids will be detected on the Gaia focal plane for a number of times between 60 and 70 on the average during the five-year operational lifetime of the mission. Even when the objects will be too faint and/or will have apparent angular sizes too small to be resolved, the disk-integrated brightness will be measured with a good accuracy. Figure 3 shows that down to magnitudes fainter than 18, even taking into account that in several cases an object, due to its motion on the focal plane, will not be measured by all nine CCD columns of the Astrometric Field, the predicted photometric accuracy for each single transit will be of the order of 0.01 mag or better. Numerical simulations strongly indicate that Gaia disk-integrated photometry will be a very important resource for asteroid studies.

Disk-integrated photometry has been historically one of the first techniques adopted to derive some important physical information about asteroids. In particular, due to the fact that asteroids are generally non-spherical objects, the amount of sunlight scattered along the direction to an observer changes with time, since the apparent illuminated cross-section as seen by the observer continually changes due to asteroid rotation. In classical asteroid photometry, the observations are carried out over time spans sufficient to obtain a so-called lightcurve, namely the full photometric variation over a whole rotation cycle of the object. From a single, good-quality lightcurve it is possible to derive an accurate measurement of the spin period of the object. When a number of lightcurves taken from the ground at different apparitions (the span of time centered around opposition, when the objects become more easily observable) are available, it is then possible to derive information about the overall shape of the object and the direction of its spin axis. The reason is that at different oppositions an object is observed in different geometric configurations with respect to the observer. In particular, the so-called aspect angle (the angle between the direction of the spin axis and the direction of the observer) changes as

a function of the ecliptic longitude at which the object is observed. Sophisticated techniques have been developed to attack the problem of the inversion of asteroid lightcurves, namely the problem of deriving the spin rate, polar axis direction and overall shape of an object based on the measurement of a sufficient number of lightcurves (Torppa et al. 2003). The results of the applications of these techniques have been largely confirmed by the in situ evidence collected by space probes (Barucci et al. 2002; Kaasalainen et al. 2002).

In the case of Gaia, the kind of photometric data that will be collected is rather different with respect to classical asteroid photometry. The main difference is that Gaia will not obtain full lightcurves, but sparse, single photometric data. This seems at a first glance a very important limit, making very hard the task of photometric inversion. How to derive the rotational and shape properties of an object having at disposal only something like 65 single photometric snapshots obtained over 5 years of time? On the other hand, these snapshots will be photometrically accurate, and homogeneous, being measured by a single detector, and not by different telescopes. In these conditions, we can think that these sparse photometric data can be considered as the single points of a time-extended hyper-light-curve, describing the photometric variation of the objects not over a single rotation period, but over a long interval of time, characterized by a continuous change of the observing circumstances, but in any case produced by the rotation of bodies around their spin axes, with the spin period, the pole direction and the body shape being constant. The problem of the inversion of data of this kind is an exciting one, and is also very timely, since in the near future not only Gaia, but also new ground-based survey telescopes like Pan-STARRS will produce this kind of data. It is then natural that different teams, including ours, have been analyzing this problem since some time. The general agreement is that sparse photometric data can be actually inverted, and will provide reliable information about the spin properties and overall shapes of the objects (Kaasalainen 2004; Durech et al. 2006).

One of the great advantages of Gaia, in particular, will be the fact of operating from space, and to be able to observe objects also at relatively small solar elongations (see Sect. 2). This means that Gaia will sample very efficiently the observations of each object in ecliptic longitude, and will therefore observe the apparent brightness over a wide interval of possible aspect angles in a relatively short time. The major drawback will be that of being forced to detect the objects not close to opposition, when they are brighter and the phase angle is smaller, but at relatively large phase angles, typically between 12 and 25°. For this reason, the variation of the magnitude of the asteroids as a function of phase angle will be important and must be taken into account. Fortunately enough, however, in the typical range of phase angles covered by Gaia observations, the variation of magnitude as a function of phase is mostly linear.

Having at disposal a number between 50 and 70 disk-integrated photometric measurement of a given object obtained over 5 years of observations, the problem is to develop an efficient inversion technique, able to determine the several unknowns of the problem, namely the spin period, the ecliptic coordinates of its rotation axis (asteroid pole), some parameters describing the overall shape of the object, the linear coefficient of the phase—magnitude relation, and an initial rotational phase corresponding to the epoch of the first observation. It must be noted, in fact, that it is convenient to work in terms of magnitude differences with respect to a given observation.

In the framework of the Gaia preparation activities, this problem has been attacked by means of a “genetic” algorithm, based on a number of simple assumptions. In particular, it is assumed that the shape of the objects can be approximated by triaxial ellipsoids, as it has been often done in the past before the development of more sophisticated lightcurve

inversion methods. Under this assumption, the shapes are simply represented by means of two parameters, corresponding to the axial ratios b/a and c/a of an ellipsoid having axes a , b , c .

The idea of a genetic algorithm is essentially that of making an efficient analysis of the space of the parameters, without producing a systematic grid exploration procedure that should be very inefficient in terms of required CPU time. Some details of the algorithm have been described by Cellino et al. (2006). The performances have been checked by means of extensive numerical simulations, which have always given very encouraging results. Even when the simulated shape is far from a regular ellipsoid, it generally turns out that the spin period and pole solution are always very good (with an accuracy better than one second in the spin period, a correct determination of the sense of rotation, and errors within 10° in pole coordinates), even if the residuals of the best solution found can be non-negligible. In other terms, the method always finds an optimal solution based on a triaxial ellipsoid assumption, and even when the residuals are not small, it turns out that the resulting spin parameters are nevertheless close to the correct solution, with small error bars derived from a statistics over different inversion attempts characterized by different initializations of the random number generation routine used by the genetic algorithm. Due to the large number of unknowns, however, and to the very simple and not realistic assumptions made, it is clear that a comparison with real data is highly desirable. This has been made recently by using the old HIPPARCOS photometric data. This is a fairly small data-set, mostly limited to some of the brightest objects belonging to the asteroid Main Belt, and affected by fairly poor photometric accuracy. The results have been very positive, however. Apart from a few exceptions, the inversion algorithm has been found to be able to find the correct solution (with errors comparable to those mentioned above for simulated tests) for the vast majority of objects with a sufficient number of HIPPARCOS photometric measurements. A paper summarizing the results of this investigation is currently in preparation. This test is very important because the HIPPARCOS data set consists of measurements similar to those that will be produced by Gaia, but much worse in terms of photometric accuracy and number of observations with respect to the expected data-set that will be produced by Gaia. This HIPPARCOS test suggests that the inversion of sparse photometric data like those that will be produced by Gaia is feasible. Since Gaia will measure with a very good accuracy all objects down to an apparent V magnitude much fainter of 18, we can expect that the Gaia photometric data set will be a very precious result of the mission. In particular, having at disposal the spin properties (rotation period and pole) for an estimated number of objects much larger than 10,000, will add a new dimension to the studies of (1) the collisional evolution of the asteroid population, (2) the efficiency of the Yarkovsky effect, (3) the YORP-driven evolution of the spin axes, and (4) the rotational properties of asteroid families, only to make a few examples (for a review of the above-mentioned Yarkovsky and YORP effects, see Bottke et al. 2002a).

Moreover, the information resulting from disk-integrated photometry about the shape and orientation of the objects at every detection, will lead to a better modeling of the asteroid signals, and of the size determination. In turn, the refinement of the asteroid signal model will lead to an improved determination of the photocenter—barycenter shift, which will permit to improve largely the accuracy of orbit determination and of the detection of subtle dynamical effects, leading to the determination of asteroid masses, Yarkovsky orbital drift and relativistic effects. This is a good example of the strong synergy of the different branches of the Gaia data reduction pipeline for the minor bodies of our Solar System.

6 Taxonomy

A new asteroid taxonomy based on the data collected by the BP and RP detectors (see Sect. 2 and Fig. 2) will be another useful result of the Gaia mission for asteroid science. In the era of the operations of the next generation of ground-based sky surveys, which will also produce massive amount of spectrophotometric data, it is clear that the Gaia spectrophotometric data alone would not be sufficient to justify a space mission. However, these data will be an extremely useful addition to the large body of information on the physical properties of these bodies, that will be produced by Gaia. For what concerns the development of a Gaia-based asteroid taxonomy, some obvious advantages must be mentioned. First, the spectrophotometric data will come from a single observing platform (no need of combining together data coming from different instruments) operating from the space (high duty cycle, no atmospheric interferences). The magnitude limit of 20 in the *V* color means that the number of detected objects will be very high, of the order of 300,000, then producing a very large sample of objects to be used to develop a new taxonomy. This is true even considering that, since asteroids have low reflectance at short wavelengths, the final sample of objects sufficiently bright to produce full spectra covering the whole wavelength interval of the BP and RP detectors will certainly be smaller than the above number of total object detections. In this respect, Fig. 10 shows the response curves of the BP and RP detectors. A major feature of these response curves is given by the fact that the Gaia spectrophotometric data of asteroids will extend down to fairly short wavelengths in the blue region of the spectrum. This is a very welcome property, because it tends to overcome one of the major limitations of recent spectroscopic surveys carried out from the ground (Bus et al. 2002), namely the fact that these surveys, including SMASS and SMASS2, have been carried out using CCD detectors with a low sensitivity in the blue. For this reason, the wavelength coverage of these surveys does not extend to wavelengths shorter than about 500 nm (Bus and Binzel 2002). As a result, several taxonomic classes that had been identified by earlier studies based on older photoelectric tube detectors, extending down to the standard U color of Johnson, are no longer distinguished by the most recent taxonomies based on more modern CCD spectra. This is a problem, because old taxonomies had identified several sub-classes of the big *C* complex which can be distinguished based on differences in their reflectance spectrum at short wavelengths. As a consequence, the future Gaia taxonomy will be very useful to study the properties of the most primitive objects, and the abundances of particular subgroups.

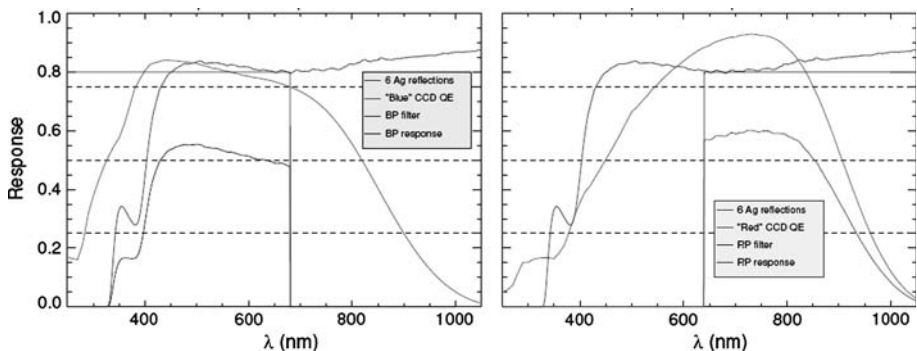


Fig. 10 Response curves of the BP and RP spectroscopic detectors of Gaia

We note also that an extensive sample of taxonomic classifications will be also extremely useful to disentangle between asteroids belonging to different dynamical families overlapping in the space of the orbital proper elements. Moreover, also the abundance of families characterized by peculiar taxonomic properties (Cellino et al. 2002) will be also systematically investigated.

Finally, we note again how the taxonomic classification will nicely complement the other kind of physical information that will be obtained by Gaia. For instance, it is worth to notice that the determination of masses, sizes and average densities for about 100 objects will be a tremendous advancement in asteroid science, also taking into account that these 100 objects will belong to different taxonomic classes. In this way, it will be possible to determine whether there are systematic differences in the average densities of bodies thought to be more or less primitive, and to possibly distinguish among different taxonomic classes also in terms of average density, to be possibly interpreted in terms of differences in average compositions and/or macroporosity.

7 Computation of Asteroid Orbits

Orbit determination and orbit improvement are central activities in the analysis and scientific exploitation of the Gaia Solar System data. There are several levels to be considered, from the preliminary orbit determination based on short arc and using simple dynamical model, up to the most extreme dynamical modeling to fit the masses or the relativistic parameters. Depending on the body (shape, surface effect, magnitude, position in the a - e plane, observation distribution) different modeling will be used during the data processing, as discussed in this section and in the next one.

The statistical orbital inversion methods consist of the non-linear least-squares method with linearized covariances (LSL; Bowell et al. 2002 and Muinonen and Bowell 1993), the Volume-of-Variation method (VoV; Muinonen et al. 2006), and orbital ranging (Ranging; Virtanen et al. 2001 and Muinonen et al. 2001). They have been developed in the framework of statistical inversion theory which aims at characterizing the full probability-density functions for the parameters of the inverse problem. For earlier reviews of their application to Gaia, see Muinonen et al. (2005) and Virtanen et al. (2005).

Typically, LSL is applicable to objects with long observational time intervals and large numbers of observations. The solution of the statistical inverse problem is specified by the least-squares orbital elements and their covariance matrix computed at the least-squares point in the orbital-element phase space. It is partly the point-estimate characteristics of LSL that limits its applicability.

VoV offers a cure to the limitations of LSL by mapping the local least-squares solutions in the phase space as a function of one or more of the parameters. The local least-squares solutions of lesser dimensions than the original one allow local sampling of orbital elements. Trial orbital elements qualify for sample elements if they produce statistically acceptable fits to the observational data. The non-linear technique complements Ranging for exiguous observational data and LSL for extensive observational data. It helps us to assess the non-linear phase transition from extended orbital-element distributions to well-constrained ones. VoV is limited by the requirement that partial derivatives need to be computed at the observation dates with subsequent matrix inversion for local covariance matrices. Should the inverse problem be poorly enough defined, VoV runs into difficulties with the matrix inversion.

Ranging offers a rigorous solution to the statistical inverse problem by exploring the full plausible orbital-element phase space for sample orbital elements. Close to the discovery epoch the observational data of an object are typically exiguous: the number of observations is very small and/or the covered orbital arc is very short. For such data, the LSL covariance matrices are seen to fail to describe the uncertainties in the orbital parameters. By exploring the topocentric ranges and angular elements (Right Ascension and Declination) at two observation dates, Ranging manages to map the full permissible region of the orbital elements without relying on partial derivatives, thus without facing numerical instabilities. Again, trial orbital elements qualify for sample elements if they produce acceptable fits to the data. Ranging gives us rigorous means to assess the uncertainties for, e.g., the dynamical classification and collision-probability assessment of near-Earth objects at their Gaia discovery epoch.

We emphasize that the global solution for asteroid orbits from Gaia data will only be ready at the end of the survey, because the asteroid dynamical evolution and physical properties are intertwined due to the precision of the Gaia astrometry. The full statistical inverse problem encompasses solving for the sizes, shapes, and masses (also for perturbing objects)—as well as relativistic effects—simultaneously for large numbers of asteroids. For statistical spin and shape inversion, see Torppa and Muinonen (2005).

For linking exiguous discovery sets of asteroid observations, we use the phase-space address-comparison method (Granvik and Muinonen 2005) which is based on Ranging and is suitable for linking observation sets needing a full orbital treatment, here particularly because of the parallax effect (Granvik et al. 2006). The key idea of the method is to compare clouds of ephemerides at several different epochs (here we have used three epochs), and require that the ephemeris clouds (using only the extent of the non-zero ephemeris p.d.f.'s) corresponding to the two observation sets that form a linkage overlap at all comparison epochs. The so-called trial linkages detected are then either accepted or discarded by computing an orbital solution based on the combined data set. We try to find an acceptable orbit by using three different methods for the orbit computation (in order of application): stepwise Ranging, simplex optimization (robust orbit improvement without the need for partial derivatives), and LSL. The linkage is accepted, if the residuals are acceptable. Note that at this stage we do not yet know whether the linkage is correct or erroneous. The correctness has to be verified by additional, archive or new observations. A similar method has also recently been developed for the identification of exiguously observed (having, say, a two-day observational arc) objects over one or more apparitions (Granvik and Muinonen 2006), which is particularly essential for inner-Earth objects detected by Gaia.

All methods described above are implemented in a completely independent software bundle called Orb. The software is written in Fortran95 using an object-oriented programming paradigm and it has been widely tested to produce correct results. At present, Orb contains some 30,000 lines of code.

Applying Ranging to simulated single-epoch Gaia data (four observations over 0.4 days) of (4) Vesta by making different assumptions for the observational noise reveals a phase transition in the uncertainty of the semimajor axis as a function of increasing observational precision (Fig. 11). Thus, even the single-epoch Gaia observations of mas-accuracy may result in reasonable orbital uncertainties. This can be important for prediction problems connected with science alerts triggered by Gaia, such as planning follow-up observations for impactor candidates.

Figure 12 shows the orbital uncertainty (obtained with LSL) at the end of the Gaia mission illustrated by the semimajor axis standard deviation as a function of the semimajor

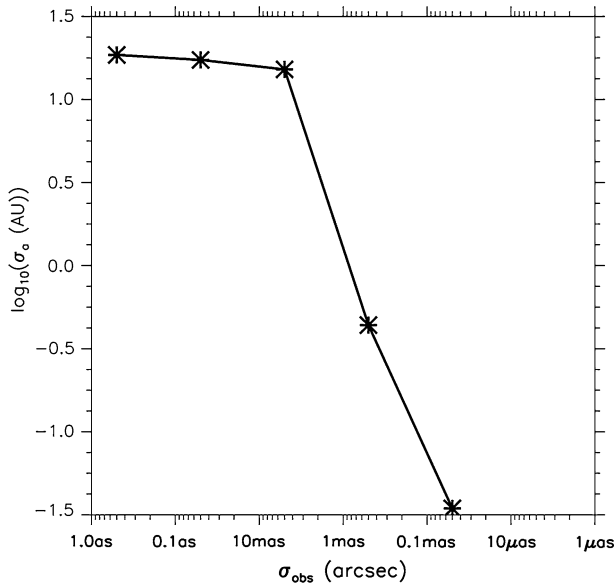


Fig. 11 Phase transition in the uncertainty of the semimajor axis as a function of improving observational uncertainty for simulated observations of (4) Vesta (four observations over 0.4 days)

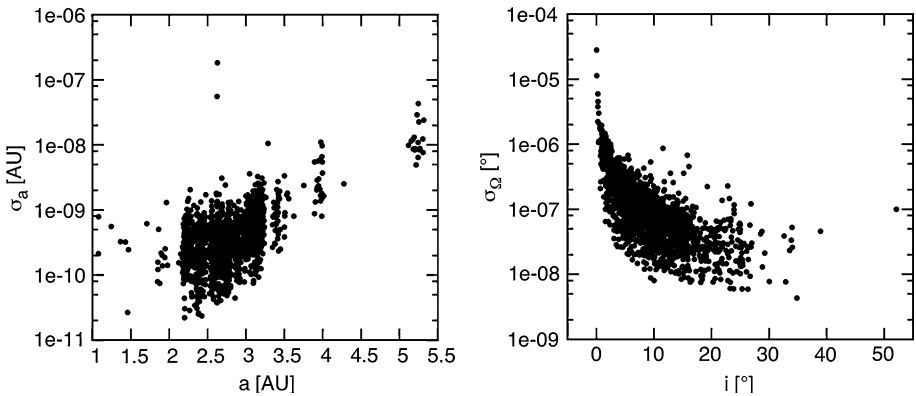


Fig. 12 The orbital uncertainty at the end of the Gaia mission illustrated by the semimajor axis standard deviation as a function of the semimajor axis (left), and by the standard deviation of the longitude of the ascending node as a function of the inclination for 1815 numbered asteroids based on simulated Gaia observations

axis (left), and by the standard deviation of the longitude of the ascending node as a function of the inclination (right) for 1815 numbered asteroids based on simulated Gaia observations. Simulated observations were generated using up-to-date information of the cadence and measurement errors, and the 2-body approximation. Note that, in the simulations, the average number of Gaia detections for each asteroid is ~ 60 , except for notorious cases such as (719) Albert (here 14 observations leading to an end-of-mission semimajor axis uncertainty of $\sim 10^{-7}$ AU for a semimajor axis of ~ 2.6 AU). As expected, the semimajor-axis uncertainty typically increases for an increasing semimajor axis, and

the uncertainty of the longitude of the ascending node increases for a decreasing inclination. Note that, when comparing Figs. 11 and 12, one must bear in mind the differing observational data.

Results based on ~ 60 simulated Gaia observations of (1) Ceres over 5 years (2-body approximation) suggest that the ephemeris uncertainty will stay below the current astrometric uncertainty (~ 0.5 arcsec) of ground-based observations for more than 600 years (Fig. 13).

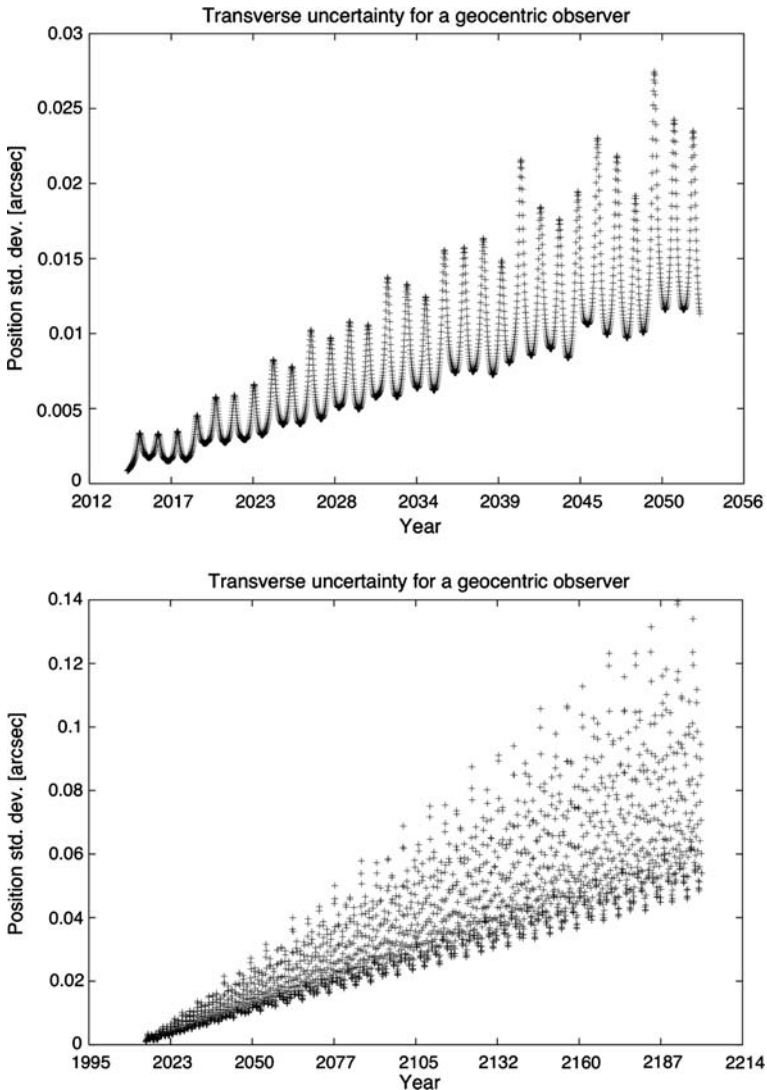


Fig. 13 The ephemeris uncertainty of (1) Ceres for a geocentric observer as function of the year. The time interval is ~ 40 years (top) and ~ 200 years (bottom). The fluctuation is due to the variable geometry between the Earth and (1) Ceres

8 Masses & Global Parameters

In this section we consider the special case of orbital fitting when additional parameters are searched for, in addition to the orbital parameters. Although the latter are determined in terms of initial conditions in the phase space, they are primarily by-products of the fit, whereas the masses or more global parameters of the reference frames are the primary targets.

The orbital period of a typical asteroid is approximately 5 years corresponding to the duration of the mission, so that the sampling in orbital longitude would generally be good as illustrated in Fig. 14, and this is an essential features in the work described here. For objects of larger orbital period (Trojans, Centaurs) or objects that are only sparsely observed by Gaia (because of their faintness or small elongation), the full orbit might be difficult to reconstruct without additional data.

Due to the scanning law peculiarities (see Sect. 2.1.1), the astrometric angles are measured on a varying great circle. Moreover, the instrumentation in the main astrometric field is such that the full spatial resolution is obtained in the along-scan direction only, and one can consider that Gaia provides one-dimensional positions, the longitudes λ on the instantaneous osculating great circle (OGC). In the linear case, when the orbit is known and only improvement is foreseen, one can write the usual Taylor expansion for the difference between the observed and computed longitudes:

$$O - C = \delta\lambda(t) = P \cdot (dx(t - \tau)) + dX(t) \approx P[\partial x/\partial q] \cdot dq + o(dq^2)$$

where $x(t)$ and $X(t)$ are the barycentric position vector of the asteroid and the Earth at time t , respectively; dq is the vector of unknown parameters including the correction to the initial conditions of the osculating orbit at a reference epoch, masses of asteroids, and other global parameters to be determined, which may affect several or all asteroids; the matrix P is the projection on the OGC. Note that the corrections to the orbit of the Earth dX can be neglected here. The precision $\sigma(dq)$ with which these parameters can be obtained has been estimated through a variance analysis.

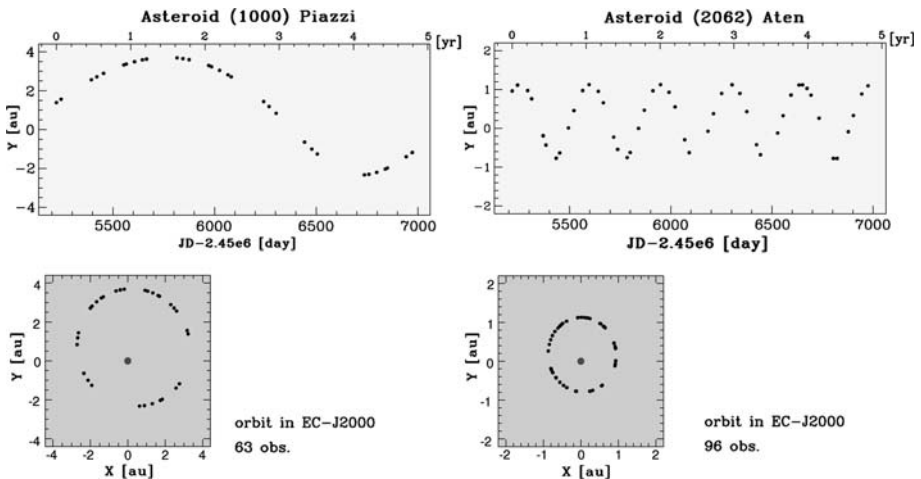


Fig. 14 Spatial and time distribution of Gaia observations for two selected asteroids. Left: one typical main-belt asteroid, 1000 Piazzi. Right: one NEA, 2062 Aten. In both cases the observations are well distributed over the 5 years duration of the mission and along the asteroid’s orbit

8.1 Mass

The asteroid mass, on a physical point of view, remains a fundamental parameter to understand the formation and evolution of these objects. When combined with the volume (i.e., size and shape that will be derived by Gaia data, see Sects. 4 and 5) it directly provides the bulk density, which is a fundamental and still poorly known parameter to interpret the internal structure and composition, and the thermal and collisional history of these objects. It is still unclear how and whether the bulk density can be directly related to the taxonomic classification (see Sect. 6), which is more intimately related to surface properties. Generally, the taxonomic classification is interpreted in terms of a comparison with meteorites collected on the ground exhibiting analogous spectral reflectance properties.

In terms of bulk density, it appears—mainly from an analysis of asteroids with satellites—that one can distinguish among three different classes: coherent, fractured, and loose asteroids, all having varying porosity of the order of 0, 25%, and 45%, respectively (Britt et al. 2002). Knowing that during a collision, the internal structure of an asteroid is affected by the propagation of a stress-wave, the porosity becomes a precious indicator of the internal structure of the asteroids and their collisional history. The comparison between the densities of objects belonging to different taxonomic classes and the density of meteorites may strengthen the evidence of a genetic relationship between different classes of meteorites and their supposed asteroid sources (Zappalà and Cellino 2002). This could provide information on the origin, formation processes and subsequent evolution of planetesimals in our Solar System.

On a dynamical point of view, knowledge of asteroid masses is needed to increase the accuracy of modern planetary ephemerides, taking into account that at present the limiting factor is the largely unknown perturbative effect of main-belt asteroids, mainly on the orbit of Mars (Standish and Fienga 2002).

There are two main ways for deriving the mass of an asteroid by means of remote observations: the analysis of the orbit of a possible satellite, or the analysis of gravitational perturbation on another asteroid during a close encounter. At present, the former is the most accurate method, and also the one which has produced so far the majority of known asteroid masses (Merline et al. 2002). Of course, this method can only be applied to those asteroids having a moon or moonlet. The other, more classical, technique (Hilton 2002) is based on the capability of measuring tiny dynamical effects, and has been so far applied only to the most massive main-belt objects.

Based on present knowledge of binaries among main-belt asteroids, Jupiter Trojans and Centaurs, Gaia will observe all known detached pairs and provide their relative positions. This will enable orbit reconstruction and, through Kepler's third law, provide the total masses of these systems. Due to the Gaia scanning law, and non-optimal sampling of the motion, orbit reconstruction for a newly discovered pair might be in principle more difficult. However, a method of preliminary orbit computation has been applied on a test case (Hestroffer et al. 2005) showing that with observations on a single apparition it should still be possible to find a good preliminary orbit, and in particular to derive the orbital period of the system. A point that has not been yet fully addressed is the possibility to detect astrometric binaries. Nevertheless, according to current simulations, the majority of asteroid mass determinations will come from measurements of close encounter perturbations.

During a close approach, and assuming for sake of simplicity a large mass ratio between the two objects, the trajectory of a small asteroid (target) is perturbed by the gravitational

pull from a bigger and more massive one (perturber), producing additional variations in the osculating elements of the target. Due to the extreme accuracy of Gaia astrometric measurements, these effects are measurable, and can be exploited to derive asteroid masses. Of course, a brute-force approach to this dynamical problem, based on the idea of integrating the full N-body problem taking into account all mutual attractions between hundreds of thousands of asteroids for five years, would be prohibitive and not necessary. Instead, it is much better to identify first all possible close encounters occurring during the Gaia operational lifetime having a significant influence on the orbits of the targets. A preliminary step has thus consisted in selecting the target asteroids from a systematic exploration of all the close approaches between perturbers and targets from 2011 to 2017. We restricted ourselves at this stage to the first 20,000 numbered asteroids as the potential targets, and considered that a potential perturber must have a mass larger than $10^{-13} M_{\odot}$ and belong to the first 2,000 numbered asteroids. A close approach is considered to be meaningful if the impact parameter b (the minimal distance between the two asteroid trajectories, where we do not take into account their mutual perturbations) is smaller than 0.5 AU and the deflection angle θ greater than 5 mas. This is evaluated with the impulse approximation as:

$$\tan(\theta/2) = G \cdot (M + m)/(v^2 b)$$

where G is the gravitational constant, M the mass of the perturber, m the mass of the target and v the relative velocity during the encounter. In a second step, the orbital motion and the partial derivatives are computed by numerical integration and the normal matrices are constructed taking advantage that we deal with a sparse Jacobian matrix. Table 1 gives the results for the precision on the mass determination out of a total of 364 potential perturbers selected using the above criterions. The results are expressed in terms of the relative accuracy $\sigma(m)/m$ where m is the reference mass used in the simulation. Then, we give the ranking of the best relative accuracies in mass determination (Table 2). We can also analyze the number of involved targets for each object mass determination, the number of close approaches for which one of the two characteristic periods (before or after the closest approach) will be out of the range of Gaia observations, the formal accuracies $\sigma(m)$, the reference masses m taken for the perturbers and the relative accuracy.

8.2 Other Global Effects

In addition to mutual close encounters and classical planetary perturbations, other forces or effects can perturb the 2-body keplerian orbit of an asteroid around the Sun, or other

Table 1 Cumulative number of derived masses in terms of relative accuracy

Number of perturbers	
Total	544
$\sigma(m)/m < 0.1\%$	2
$\sigma(m)/m < 1\%$	7
$\sigma(m)/m < 10\%$	42
$\sigma(m)/m < 15\%$	56
$\sigma(m)/m < 20\%$	76
$\sigma(m)/m < 30\%$	113
$\sigma(m)/m < 50\%$	150

Table 2 Formal precisions for the 10 best-determined masses, in order of decreasing precision

N°	Name	σ (m)	Mass m	$\sigma(m)/m$
4	Vesta	9.29×10^{-14}	1.30×10^{-10}	0.07
1	Ceres	3.50×10^{-13}	4.50×10^{-10}	0.08
14	Irene	1.03×10^{-13}	2.60×10^{-11}	0.40
27	Euterpe	5.14×10^{-14}	1.00×10^{-11}	0.51
10	Hygiea	3.25×10^{-13}	4.70×10^{-11}	0.69
52	Europa	2.19×10^{-13}	2.40×10^{-11}	0.91
2	Pallas	1.28×10^{-12}	1.30×10^{-10}	0.98
15	Eunomia	2.79×10^{-13}	3.00×10^{-11}	1.86
46	Hestia	2.25×10^{-14}	1.20×10^{-12}	1.88
511	Davida	6.17×10^{-13}	3.00×10^{-11}	2.06

solar-system targets observed by Gaia. Some examples are given by the Yarkovsky effect affecting relatively small bodies (Bottke et al. 2002a), outgassing jets affecting comets (known or hidden in the main-belt of asteroid), mutual perturbations of planetary satellites, etc. Here, we will discuss the role played by relativistic effects on the orbit of an asteroid considered to be a test particle. General Relativity (GR) predicts a precession of the perihelion for any object orbiting in the gravitational field of the Sun. Historically, the first proof of this effect was given by the successful explanation of the anomalous drift of Mercury’s perihelion.

General Relativity is one particular case of a larger class of metric theories of relativity that can be gathered in one parameterized formulation in cases of weak gravity fields and low velocities, namely the parameterized post-Newtonian (PPN) formalism. The most important PPN parameters for our purposes are β , all being equal to one in GR. Tests of GR can hence be obtained by measuring these parameters, and their possible deviations from unity (e.g., Will 2006). Some attempts have been done by means of observations of the near-Earth asteroid 1766 Icarus, but with little success, mainly due to large observational and systematic errors (e.g., Gilvary 1953; Shapiro 1971; Sitarski 1992). Considering that the parameter γ is obtained by measuring the light deflection of stars with high accuracy, the precession of an asteroid’s perihelion $d\omega$ is mainly a function of two unknowns, namely the parameter β and the solar quadrupole J_2

$$\begin{aligned} \delta\omega &= \delta\omega_{\text{PPN}} + \delta\omega_{J_2} \\ &= [6\pi m_{\odot} a^{-5/2} (1 - e^2)^{-1} (2 + 2\gamma - \beta) / 3 + 6\pi R_{\odot}^2 a^{-7/2} (1 - e^2)^{-2} (5 \cos^2 i - 1) / 4] \\ &\quad \cdot (\tau - \tau_o) \end{aligned}$$

where $m_{\odot} \approx 1.48$ km.

These parameters cannot be separated when observing a single body, e.g., Mercury or Icarus, and one needs to assume either β from, e.g., LLR, or the solar J_2 from heliosismology. By observing with high accuracy a large number of test particles of various semi-major axes and eccentricities, Gaia will enable to better separate these two parameters and provide direct and simultaneous determination of both of them¹. A test has been successfully carried out on a simulated population of near-Earth asteroids (Bottke et al.

¹ The effects induced by the Sun’s quadrupole on the precession of the node—which is not reproduced here—and the mean motion give additional constraints.

Table 3 Formal precision on parameters fitting for the test of General Relativity, the solar J2, the secular change of the gravitational constant and the link of the dynamical frame to the ICRF represented by the rotational shift at the reference epoch and its first derivative, that is to say the residual spin of the dynamical frame relative to the kinematically non-rotating frame based on predictions for 300,000 asteroids

Parameter	β —	J ₂ —	G ⁻¹ .dG/dt year ⁻¹	Wo μ as	dW/dt μ as/year
1 σ precision	5×10^{-4}	2×10^{-7}	2×10^{-12}	1.5–1.5–5	0.5–0.5–1.5

2002b) that should be complete up to magnitude $V \leq 20$, and a subset of 20,000 main-belt asteroids. Since Gaia will observe an even larger number of asteroids (of the order of 300,000, see Sect. 1.2), one can expect a further improvement on the precision of the constant of gravity and reference frame linking. Expected results in term of the precision of this test are given in Table 3.

Interestingly, some highly eccentric NEAs can be as much sensitive to this effect as Mercury, and even more if one considers some possible transient body with extremely large eccentricity on his way to fall onto the Sun (Farinella et al. 1994).

Finally, all positions of asteroids are computed in a dynamical reference frame that is materialized by a plane of reference and an origin which are commonly given by a mean ecliptic and equinox for a given epoch (J2000). On the other hand, all observed positions are given with respect to the QSOs on the celestial sphere materializing a kinematically non-rotating reference frame. The optical counterpart of the International Celestial Reference Frame (ICRF) will be directly given by Gaia from direct observations of selected QSOs. Comparison of the computed and observed positions yields the link between the dynamical reference frame and the ICRF (e.g., Standish 1998; Chapront et al. 2002). Similarly, one can derive such rotation from the observations of all asteroids observed by Gaia, and test the presence of a possible rotation rate to the level of about 10^{-11} rad/year (see Table 3).

9 Relations with Ground-based Observations

At the present time, thousands of asteroids are regularly discovered from ground-based surveys. As mentioned in Sect. 2.2, if one considers the current increasing rate of discoveries and the limiting magnitude of present and future surveys (e.g., Pan-STARRS), it is not clear how many new objects will remain to be discovered at the time of the Gaia mission, probably a few. Nevertheless, Gaia will systematically observe the whole sky, including the crowded galactic plane, high inclination zones, and also the regions at small solar elongations (45° , see Fig. 6, to be compared for instance with the 60° of the Hubble Space Telescope). This makes it a survey more efficient than any ground-based survey for discovering relatively bright objects that spend most of their time inside the orbit of the Earth such as Atens and Inner-Earth orbiters (IEOs, see Michel et al. 2005). These objects are extremely interesting, since only a few of them have been discovered so far, and they also include potentially hazardous objects that can avoid detection from the ground for a very long time. Once any object of this kind will be discovered, it will surely be profitable—if not necessary—to have an immediate follow-up from the ground, to avoid losing it either because it is not observable or too faint.

The observational data from the Gaia observatory will be regularly downloaded to the ground-segment. A first cross-matching will be applied to them. All the observations that do not correspond to any known object will be kept apart. Objects exhibiting a motion

suggesting an Aten or IEO orbit will be made public in order to set up possible ground-based recovery and follow-up. Eventually, at the end of the mission the whole set of previously unknown objects detected by Gaia will be processed to identify the linkings among different observations of the same objects, in order to derive the orbits of these newly discovered bodies. At that stage, the linked detections will be reprocessed by the whole pipeline of routines for physical characterization.

Finally, in addition to all the science achievable from direct Gaia observations of Solar System objects, from the point of view of future ground-based observations (not in alert mode), one should keep in mind that the Gaia stellar catalogue will provide a precious basis for all future astrometric observations, including, as a first possible application, the accurate prediction of future stellar occultations by Solar System objects.

10 Conclusions

In many respects, Gaia represents the most effective tool we can imagine to derive essential physical and dynamical information on the asteroids and other kinds of minor bodies of our Solar System by means of remote observations. In some respects, Gaia is an extension of the observing facilities currently existing on the ground, but taking full profit of the advantage of observing from space. In this sense, Gaia may be seen as an excellent example of a synergy between classical remote sensing by means of optical telescopes, and space missions able to derive details that cannot be obtained from the ground.

Gaia will be launched in 2011, according to the current schedule of the ESA. Up to that date, we will be involved in the frantic activities that always are related to the preparation of a space mission. There is always some risk related to the launch of satellites or interplanetary probes. Although we are aware of this, and we keep our fingers crossed, we think that the know-how we are developing during these years, represents in any case an excellent investment of time, since the success of Gaia or even another possible mission of this kind will trigger a real revolution in our knowledge of the minor bodies in our Solar System, by exploiting up to their current limits remote sensing techniques that are still essential even today, in the era of spectacular in situ exploration of single bodies by means of space probes.

Acknowledgements We thank the Gaia DPAC (Data Processing and Analysis Consortium) for providing several Figures of the Gaia instrumental set-up. This work is the product of many interactions and discussions among a large number of scientists (too many to be listed here) involved in the former Gaia Solar System Working Group. In particular, some parts of this paper have been improved thanks to the help of J. Berthier, J. Frouard, B. Balat.

References

- M.A. Barucci, A. Cellino, C. De Sanctis, M. Fulchignoni, K. Lumme, V. Zappalà, P. Magnusson, Ground-based Gaspra modelling - Comparison with the first Galileo image. *Astron. Astrophys.* **266**, 385–394 (2002)
- U. Bastian, M. Biermann, Astrometric meaning and interpretation of high-precision time delay integration CCD data. *Astron. Astrophys.* **438**, 745–755 (2005)
- W.F. Bottke, D. Vokrouhlický, D.P. Rubincam, M. Broz, in *Asteroids III*, ed. by W.F. Bottke, A. Cellino, P. Paolicchi and R.P. Binzel (University of Arizona Press, 2002a), pp. 395–408.
- W.F. Bottke, A. Morbidelli, R. Jedicke, J.M. Petit, H.F. Levison, P. Michel, T.S. Metcalfe, Debiased orbital and absolute magnitude distribution of the near-earth objects. *Icarus*. **156**, 399–433 (2002b)

- D.T. Britt, D. Yeomans, K. Housen, G. Consolmagno, in *Asteroids III*, ed. by W.F. Bottke, A. Cellino, P. Paolicchi, R.P. Binzel (University of Arizona Press, 2002), pp. 485–500
- E. Bowell, J. Virtanen, K. Muinonen, A. Boattini, in *Asteroids III*, ed. by W.F. Bottke, A. Cellino, P. Paolicchi, R.P. Binzel (University of Arizona Press, 2002), pp. 27–45
- S.J. Bus, R.P. Binzel, Phase II of the small main-belt asteroid spectroscopic survey: a feature-based taxonomy. *Icarus*. **158**, 146–177 (2002)
- S.J. Bus, F. Vilas, M.A. Barucci, Visible-wavelength spectroscopy of asteroids, in *Asteroids III*, eds by W.F. Bottke, A. Cellino, P. Paolicchi, R.P. Binzel (University of Arizona Press, Tucson, 2002), pp. 169–182
- A. Cellino, S.J. Bus, A. Doressoundiram, D. Lazzaro, in *Asteroids III*, ed. by W.F. Bottke, A. Cellino, P. Paolicchi, R.P. Binzel (University of Arizona Press, 2002), pp. 633–644
- A. Cellino, M. Delbò, V. Zappalà, A. Dell’Oro, P. Tanga, Rotational properties of asteroids from GAIA disk-integrated photometry: a “Genetic” algorithm. *Adv. Space Res.*, **38**, 2000–2005 (2006)
- J. Chapront, M. Chapront-Touzé, G. Francou, A new determination of lunar orbital parameters, precession constant and tidal acceleration from LLR measurements. *Astron. Astrophys.* **387**, 700–709 (2002)
- A. Dell’Oro, A. Cellino, Asteroid sizes from Gaia observations, in *Proceedings of the Symposium Three Dimensional Universe with Gaia (ESA SP-576)*, p. 289 (2005)
- J. Durech, T. Grav, R. Jedicke, L. Denneau, M. Kaasalainen, Asteroid models from the Pan-STARRS photometry. *Earth Moon Planet.* **97**(3–4), 179–187 (2006)
- P. Farinella, Ch. Froeschlé, C. Froeschlé, R. Gonczi, G. Hahn, A. Morbidelli, G.B. Valsecchi, Asteroids falling onto the Sun, *Nature*, **371**, 315–317 (1994)
- J.J. Gilvary, *Phys. Rev.* **89**, 1046 (1953)
- M. Granvik, K. Muinonen, Asteroid identification at discovery, *Icarus*. **179**, 109–127 (2005)
- M. Granvik, K. Muinonen, Near-earth object identification over apparitions using n-body ranging, in *Proceedings of IAU Symposium #236: “Near Earth Objects, our Celestial Neighbors: Opportunity and Risk”* (American Astronomical Society, DPS meeting #39, #50.11, 2006)
- M. Granvik, K. Muinonen, L. Jones, B. Bhattacharya, M. Delbo, L. Saba, A. Cellino, E. Tedesco, D. Davis, V. Meadows, Linking Large-Parallax Spitzer-CFHT-VLT observations of asteroids. *Icarus* **192**(2), 475–490 (2006)
- D. Hestroffer, F. Vachier, B. Balat, Orbit determination of binary asteroids. *Earth Moon Planet.* **97**, 245–260 (2005)
- J.L. Hilton, in *Asteroids III*, ed. by W.F. Bottke, A. Cellino, P. Paolicchi, R.P. Binzel (University of Arizona Press, 2002), pp. 103–112
- M. Kaasalainen, Physical models of large number of asteroids from calibrated photometry sparse in time. *Astron. Astrophys.* **422**, L39–L42 (2004)
- M. Kaasalainen, S. Mottola, M. Fulchignoni, in *Asteroids III*, ed. by W.F. Bottke, A. Cellino, P. Paolicchi, R.P. Binzel (University of Arizona Press, 2002), 139
- L. Lindegren, A three-step procedure for deriving positions, proper motions, and Parallaxes of stars observed by scanning great circles. Technical Note, Lund Observatory, Oct 1976. (1976)
- W.J. Merline, S.J. Weidenschilling, D.D. Durda, J.L. Margot, P. Pravec, A.D. Storrs, in *Asteroids III*, ed. by W.F. Bottke, A. Cellino, P. Paolicchi, R.P. Binzel (University of Arizona Press, 2002), pp. 289–314
- P. Michel, V. Zappalà, A. Cellino, P. Tanga, Estimated abundance of atens and asteroids evolving on orbits between earth and sun. *Icarus*. **143**, 421–424 (2000)
- K. Muinonen, E. Bowell, Asteroid orbit determination using Bayesian probabilities, *Icarus*. **104**, 255 (1993)
- K. Muinonen, J. Virtanen, E. Bowell, Collision probability for earth-crossing asteroids using orbital ranging, *CMDA* **81**, 93–101 (2001)
- K. Muinonen, J. Virtanen, G. Granvik, T. Laakso, Asteroid orbits with Gaia: inversion and prediction. in *Proceedings of the Symposium Three Dimensional Universe with Gaia (ESA SP-576)*, pp. 223–230 (2005)
- K. Muinonen, J. Virtanen, M. Granvik, T. Laakso, Asteroid orbits using phase-space volumes of variation, *MNRAS*, **368**, 809–818 (2006)
- I.I. Shapiro, W.B. Smith, M.E. Ash, S. Herrick, General relativity and the orbit of Icarus, *Astron. J.* **76**, 588 (1971)
- G. Sitarski, On the relativistic motion of (1566) Icarus, *Astron. J.* **104**, 1226–1229 (1992)
- M. Standish, Linking the dynamical reference frame to the ICRF, *Highlights Astron.* **11**, 310 (1998)
- M. Standish, A. Fienga, Accuracy limit of modern ephemerides imposed by the uncertainties in asteroid masses. *Astron. Astrophys.* **384**, 322–328 (2002)
- J. Torppa, M. Kaasalainen, T. Michalowsky, T. Kwiatkowsky, A. Kryszczyńska, P. Denchev, R. Kowalsky, Shapes and rotational properties of thirty asteroids from photometric data. *Icarus*, **164**, 346–383 (2003)
- J. Torppa, K. Muinonen, Statistical inversion of Gaia photometry for asteroid spins and shapes. in *Proceedings of the Symposium Three Dimensional Universe with Gaia (ESA SP-576)*, pp. 321–324 (2005)

- F. van Leeuwen, The HIPPARCOS mission, *Space Sci. Rev.* **81**, 201–412 (1997)
- F. van Leeuwen, Rights and wrongs of the Hipparcos data. A critical quality assessment of the Hipparcos catalogue. *Astron. Astrophys.* **439**, 805–822 (2005)
- J. Virtanen, K. Muinonen, E. Bowell, Statistical ranging of asteroid orbits. *Icarus* **154**, 412 (2001)
- J. Virtanen, K. Muinonen, F. Mignard, Asteroid orbits with Gaia: simulated examples. In *Proceedings of the Symposium Three Dimensional Universe with Gaia (ESA SP-576)*, pp. 325–328. (2005)
- C. Will, The confrontation between general relativity and experiment, *Living Rev Relativity*, **9**, 3 (2006)
- V. Zappalà, A. Cellino, in *GAIA: an european space project*, ed. by O. Bienaymé, C. Turon, EAS Publications Series vol. 2, p. 343 (2002)